Journal of Sciences, Islamic Republic of Iran 23(4): 313-318 (2012) http://jsciences.ut.ac.ir
University of Tehran, ISSN 1016-1104

Synthesis and Characterization of V_2O_5/SiO_2 Nanoparticles as Efficient Catalyst for Aromatization 1,4 Dihydropyridines

F. Farzaneh,[1,*] E. Zamanifar,[1] L. Jafari Foruzin,[1] and M. Ghandi[2]

[1]*Department of Chemistry, Faculty of Sciences, University of Alzahra, P.O.Box 1993891176, Vanak, Tehran, Islamic Republic of Iran*
[2]*School of Chemistry, Colloge of Science, University of Tehran, P.O. Box, 14155-6455, Tehran, Islamic Republic of Iran*

Received: 20 June 2012 / Revised: 29 December 2012 / Accepted: 7 January 2013

Abstract

V_2O_5/SiO_2 nanoparticles was prepared via an one-pot sol gel method from vanadyl- acetylacetonate and tetraethylorthosilicate in refluxing MeOH, followed by calcination at 700 °C for 2 hours. The resultant nanoparticles was characterized by means of scanning electron microscopy (SEM), transmission electron microscopy (TEM), X-ray diffraction (XRD), TGA and FTIR techniques. Rapid and efficient aromatization of 1,4-dihydropyridines (DHPs) catalyzed by V_2O_5/SiO_2 nanoparticles is described in this presentation.

Keywords: V_2O_5/SiO_2 nanoparticles; Aromatization; 1,4-Dihydropyridines; Acetic acid

Introduction

Although there has been many reports on the preparation and characterization of nanomaterials based on the metal and mixed metal oxides in recent years [1], a few reports on the V_2O_5/SiO_2 mixed oxides as nanoparticles are available in literature [2]. Catalysis systems based on the supported vanadium oxide exhibit interesting catalytic properties for the partial oxidation of alkanes, aromatics, alcohols, and alkenes and dehydrogenation of different hydrocarbons [3-5].

DHPs are analogues of nicotinamide adenine dinucleotide hydride (NADH) coenzyme [6]. It has been found that NADH initially undergoes oxidative aromatization to the corresponding pyridine derivative during the metabolism by the action of Cytochrome P-450, present in liver [7]. As indicated in Figure 1, some pyridine derivatives such as **1**, **2** and **3**, are medicinally significant compounds and used as selective human adenosine receptor modulators [8], protein kinase C (PKC) inhibitor [9] or for treatment of atherosclerosis and other coronary diseases, respectively [10]. To understand the biological processes of poly-substituted pyridines, these compounds have been prepared via different procedures, amongst which oxidative aromatization of 1,4-DHPs have attracted the chemist's attention for the discovery of new preparation methods in recent years. Numerous oxidants such as nitrogen oxides [11], metallic nitrates [12], CrO_2 [13], $KMnO_4$ [14], SeO_2 [15], $Pb(OAc)_4$ [16], Co-naphthenate/O_2 [17], palladium catalysts [18], hypervalent iodine reagents [19], solid acids [20], cytochrome P-450 [21], iron(III) phthalocyanine chloride [22], vanadium salts [23] and many other reagents have been used for the

* Corresponding author, Tel.: +98(21)8825897, Fax: +98(21)88041344, E-mail: faezeh_farzaneh@yahoo.com

aromatization of 1,4-DHPs. Herein, we report the one-pot synthesis and characterization of V_2O_5/SiO_2 nanoparticles via a sol-gel method from vanadyl acetylacetonate and tetraethylorthosilicate and its application as catalyst for oxidative aromatization of Hantzsch 1,4-DHPs to the corresponding substituted pyridines.

Materials and Methods

Materials and Instrumentation Details

All chemicals and reagents were of synthetic grade and used without further purification.

X-ray powder diffraction (XRD) data were recorded on a diffractometer type, Seifert XRD 3003 PTS, using Cu kα_1 radiation (λ = 1.5406 Å). The nanostructures of the sample were analyzed by scanning electron microscopy (SEM; S-4160 Hitachi) and transmission electron microscopy (TEM; Philips EM 208s) at an accelerating voltage of 100 KV. Thermal studies were performed using mettler-toledo TGA/SDTA-851. FT-IR spectra were recorded on a Bruker Tensor 27 FTIR spectrometer. Oxidative aromatization products were analyzed by GC and GC-MS using an Agilent 6890 Series with FID detector, HP-5, 5% phenylmethyl-siloxane capillary and an Agilent 5973 Network, mass selective detector, HP-5 MS 6989 Network GC system, respectively.

Preparation of V_2O_5/SiO_2 Nanoparticles

Tetraethylorthosilicate (TEOS) (3.2 mL) was added to a solution containing vanadium acetylacetonate (0.18 g) in MeOH (20 mL) under stirring at room temperature. The pH of the prepared solution was then adjusted to 11 by addition appropriate amount of NH_4OH. The generated green solution was then refluxed for 48 h. The final solid product was filtered, washed with hot MeOH, and dried at 60° C. It was finally calcined at 700°C for 2 h. The V and Si content of the resultant nanomaterials were found to be 9.1 and 75.9%, respectively.

Aromatization of Hantzsch 1,4 DHPs with V_2O_5/SiO_2 Nanoparticles: General Procedure

A suspension of 1,4-DHPs [24] (0.03 mmol) and V_2O_5/SiO_2 nanoparticles (8 mg) in acetic acid (15 mL) was stirred at 40° C. The progress of the reaction was monitored by TLC. After completion of the reaction, the mixture was poured into H_2O (15 mL) and the aqueous solution was then extracted with CH_2Cl_2 (15 mL). The organic layer was dried with anhydrous sodium sulphate and filtered. The filtrate was concentrated at reduced pressure before subjecting to GC and GC-Mass analysis.

Results and discussion

Characterization of Nanoparticles

Typical SEM image of the V_2O_5/SiO_2 mixed oxides, calcined at 700° C for 2 h, depicted in Fig. 2a, shows nanoparticles. Characterization with more details was

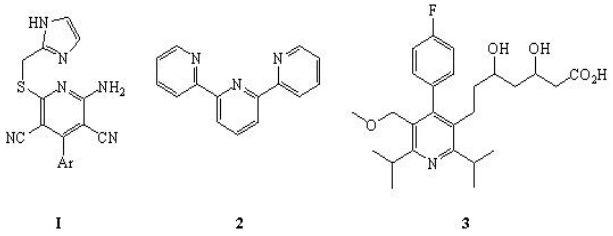

Figure 1. Some pyridine derivatives as significant medicines.

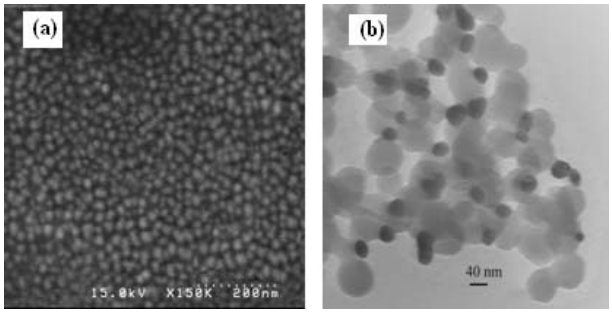

Figure 2. SEM (a) and TEM (b) images of V_2O_5/SiO_2 mixed oxides nanoparticles.

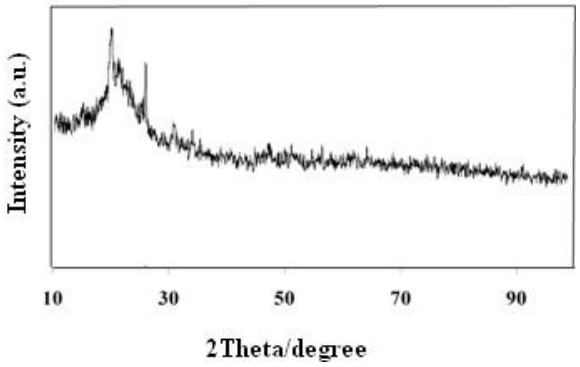

Figure 3. The XRD pattern of V_2O_5/SiO_2 mixed oxides nanoparticles.

carried out by TEM. As seen in Fig. 2b, the V_2O_5 nanoparticles are located on the amorphous SiO_2 network.

Powder X-ray diffraction (PXRD) pattern of V_2O_5/SiO_2 nanoparticles, after thermal treatment at 700°C in air is shown in Fig. 3. The pattern observed in a broad band in the region of 2Θ 20-30 ° is attributed to the amorphous silica matrix. Despite the amount of V_2O_5, some low intensity diffraction peaks related to the V_2O_5 supported on the amorphous silica pattern are observed.

The FTIR spectra of the V_2O_5/SiO_2 nanoparticles before and after calcination at 700° C are shown in Fig. 4a and 4b respectively. The bands observed at 3440 and 1627 cm^{-1}, due to the OH stretching and bending vibrations (Fig. 4a) appear with lower intensities after calcinations because of loosing solvent molecules and condensation of the lattices (Fig. 4b). The bands displaying at 1381 cm^{-1} along with a sholder at 1035 cm^{-1} (Fig. 4a), due to the asymmetric and symmetric Si-O-Si vibrations, shift to 1110 cm^{-1} after calcinations (Fig. 4b). Since the spectra are dominated by SiO_2 framework vibrations, the characteristic vibration modes of the vanadium pentoxide [25-26] are not clearly evident. Interestingly, four peaks at 1110, 934, 806 and 471 cm^{-1} due to the Si-O-Si and Si-O-V vibrations are observed in the calcined catalyst (Fig. 4b). The similarity of the FTIR spectrum of the used V_2O_5/SiO_2 nanoparticles (Fig. 4c) with that of the unused catalyst (Fig. 4b) is of particular significance. Therefore, the reusability of V_2O_5/SiO_2 nanoparticles as catalyst in other reactions is not surprising (vide infra).

Fig. 5 exhibits the Raman spectrum of V_2O_5/SiO_2 mixed oxides nanoparticles in the range of 1200-200 cm^{-1}. The observed typical bands of crystalline V_2O_5 at 1015, 685, 518, 311, 278 and 128 cm^{-1} are consistent with those reported before [26,27].

The thermogravimetric (TGA) and DTA curves of V_2O_5/SiO_2 nanoparticles before thermal treatment in air was prepared in the range of 25 to 700°C (Fig. 6). The weight loss (approximately 7.52%) up to 200°C, observed by careful inspection of the TGA and DTA can be attributed to the removal of weakly–bounded solvent molecules in nanoparticles pores. TGA analysis also shows a continuous weigh loss (approximately 11.63%) up to 850 °C, corresponding either to the loss of more strongly bounded solvent molecules or decomposition of the unreacted alkoxide groups. In the DTA curve, the observed exothermic peaks in the range of 300-500°C is assigned to an exothermic combustion of organic compounds such as tetraethylorthosilicate ethyl groups or acetylacetone.

Catalytic Activity

The prepared V_2O_5/SiO_2 nanoparticles as a new environmentally benign and effective catalyst was used for aromatization of Hantzsch 1,4-DHPs. Initially, the

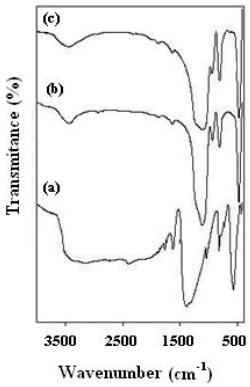

Figure 4. The FTIR spectra of V_2O_5/SiO_2 mixed oxides nanoparticles (a) as prepared, (b) after calcinations at 700° C and (c) reused as catalyst.

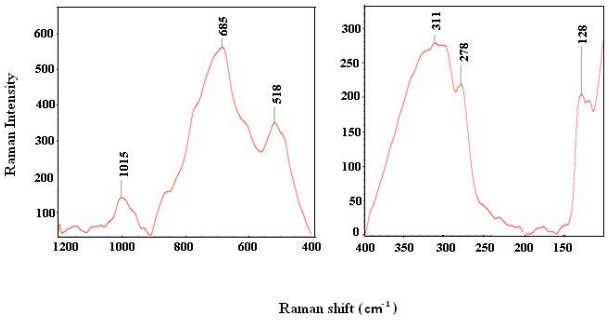

Figure 5. Raman spectra of V_2O_5/SiO_2 mixed oxides nanoparticles in the range 1200-400 and 400-150 cm^{-1}.

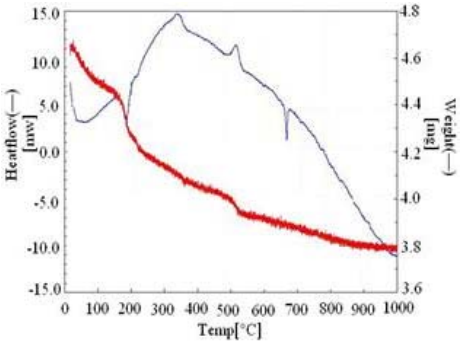

Figure 6. The TGA/ DTA of V_2O_5/SiO_2 mixed oxides nanoparticles.

DHPs **3a**, **3b**, and **3c** were prepared according to the previously reported procedure (Scheme 1A) [24]. In the model experiment, it was found that 40% of **3a** is selectively converted to the corresponding aromatic derivative **4a** in 7 min, when stirring in acetic acid, a commonly solvent used in the aromatization of 1,4-DHPs (Scheme 1B, Table 1, entry 1). **3a** Conversion to **4a** was increased to 95, 97% and 100% when the reaction time was extended to 9, 11 and 13 min (Table 1, entries 2, 3 and 4).

To optimize the reaction conditions, effect of the amount of catalyst was examined (Table 2). As illustrated in Table 2, increasing the amount of the catalyst from 2 to 8 mg increased the conversion of **3a** to **4a** from 92% to 100% (Table 2, entries 1-4).

Results of the effect of solvent on the conversion of **3a** to **4a** is presented in Table 3. Compared to CH_3CO_2H (Table 3, entry 1), reactions were sluggish in CH_3CO_2 Et-H_2O_2, a commonly solvent mixture frequently used in catalytic aromatization of 1,4-DHPs (Table 3, entries 2 and 3). Similarly, the aromatization reaction proceeded slowly in CCl_4 (Table 3, entry 4). Reactions were inefficient either with SiO_2 void of V_2O_5 or in the absence of catalyst (Table 3, entries 5 and 6). Therefore, the presence of V_2O_5/SiO_2 nanoparticles as catalyst was found to have a vital role on the conversion of 1,4-DHPs to the corresponding aromatic analogues.

The established optimized reaction conditions were then tested on **3b** and **3c** (Scheme 1B). We have included the result obtained for **3a** in Table 4 in order to make the comparison with **3b** and **3c** more convenient. As indicated in Table 4, **4b** and **4c** were obtained quantitatively in 5 and 11 min (Table 4, entries 2 and 3). Compared to **3a** (Table 4, entry 1), conversion of either **3b** or **3c** have taken place more efficiently. The observed rate enhancement trend by changing the Ph to Me and H is in accord with the decreasing steric hindrance at the substituted carbon. Such trend is not unexpected since approaching rate of the active catalyst for removal of the bis-allylic H atom located next to Ph, Me or H groups increases with the decreasing steric hindrance at the bis-allylic carbon.

Notably, utilization of the used V_2O_5/SiO_2 nanoparticles as catalyst in the second and third aromatization reactions of **3a** proceeded selectively to **4a** with 95% and 89% conversions, respectively. Finally, the chemical analysis of the reaction filtrate showed that about 0.2% of vanadium has been lost from the catalyst during the reactions. Accordingly, the FT-IR spectrum of the recovered V_2O_5/SiO_2 nanoparticles (Fig. 4c) was similar to that of the freshly prepared catalyst (Fig. 4a). These evidences clearly indicate the reusability and stability of our prepared catalysis system.

Table 1. Effect of time on the aromatization[a] of **3a**

Entry	Time (min)	Conversion (%)	Selectivity (%)
1	7	40	100
2	9	95	100
3	11	97	100
4	13	100	100

[a]Conditions: **3a** (0.03 mmol), catalyst: V_2O_5/SiO2 (8 mg), solvent: acetic acid (15 mL).

Table 2. Effect of the amount of catalyst on aromatization[a] of **3a**

Entry	Catalyst Amount (mg)	Conversion (%)	Selectivity (%)
1	2	92	100
2	4	93	100
3	6	98	100
4	8	100	100

[a]Conditions : **3a** (0.03 mmol), time: 13 min, catalyst: V_2O_5/SiO2 (8 mg), solvent : acetic acid (15 mL).

Table 3. Effect of solvent on the aromatization of **3a**

Entry	Solvent	Time (min)	Conversion (%)	Selectivity (%)
1	CH_3CO_2H[a]	13	100	100
2	CH_3CO_2Et[a] H_2O_2[b]	660	50	100
3	CH_3CO_2Et[a] H_2O_2[b]	1440	100	100
4	CCl_4[a]	1440	20	100
5	CH_3CO_2H[c]	1440	-	-
6	CH_3CO_2H[d]	1440	2	100

[a]Conditions : [a]Conditions : **3a** (0.03 mmol), time: 13 min, catalyst: V_2O_5/SiO2 (8 mg), solvent : acetic acid (15 mL). [b]0.5 mL, 30%, [c]SiO_2 (8 mg) was used as catalyst, solvent (15 mL), [d]No catalyst was used, solvent (15 mL).

Table 4. The Effect of substituent on the aromatization[a] of 1,4-DHPs

Entry	DHP	Time (min)	Conversion (%)	Selectivity (%)
1	**3a**	13	100	100
2	**3b**	5	100	100
3	**3c**	11	100	100

[a]Conditions : **3a** (0.03 mmol), catalyst: V_2O_5/SiO2 (8 mg), solvent: acetic acid (15 mL).

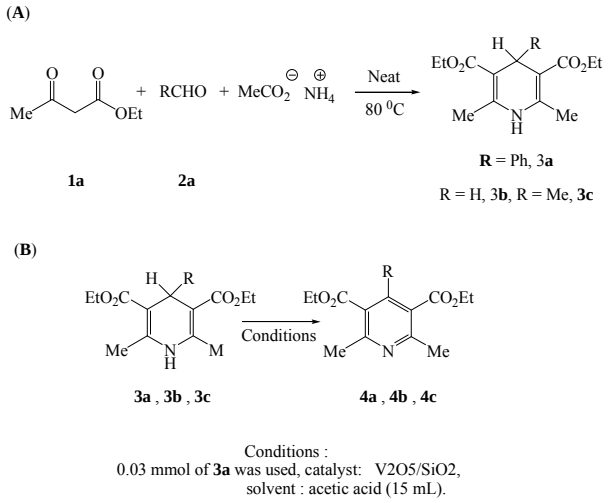

Scheme 1. (A) Synthesis of 1,4-DHPs, (B) catalytic aromatization of 1,4-DHPs.

In summary, an expedient synthetic procedure for the preparation of V_2O_5/SiO_2 nanoparticles, via a sol-gel process was reported in this presentation. Utilization of no surfactant or any other template is the novelty of this method. The synthetic route described herein implies an improved method for the preparation of a composite material. The V_2O_5 nanoparticles, located on the silica matrix was tested as catalyst for the aromatization of Hantzsch 1,4 DHPs. A number of DHPs were quantitatively converted to the corresponding aromatic analogues in short reaction times. Overall, the simplicity of the method, easy preparation, reusability and stability of the catalyst, along with the mild reaction conditions, and quantitative conversion of the used Hantzsch DHPs to the desired products are some advantages of our procedure.

Acknowledgement

This work was financially supported by the University of Alzahra.

References

1. Ferna´ndez-Garcia, M. Martinez-Arias, A. Hanson, J. C. Rodriguez, J.A. Nanostructured oxides in chemistry: characterization and properties. Chem. Rev. **104:** 4063-4104 (2004).
2. Moreau, J. J. E. Man, M. W. C. The design of selective catalysts from hybrid silica-based Materials. Coord. Chem. Rev. **178-180:** 1073-1082 (1998).
3. Weckhuysen, B. M. Keller, D. E. Chemistry, spectroscopy and the role of supported vanadium oxides in heterogeneous catalysis. Catal. Today **78**: 25–46 (2003).
4. Neumann, R. Leavin-Elad, M., Vanadium silicate xerogels in hydrogen peroxide catalyzed oxidations. Appl. Catal. A, **122:** 85-97(1995).
5. Bottino, A. Capannelli, G., Comite, A., Storace, S. Di Felice, R. Kinetic investigations on the oxidehydrogenation of propane over vanadium supported on Al_2O_3 Chem. Eng. J. **94:** 11-18 (2003).
6. Mauzeral, D. Westheimer, F. H. 1-Benzyldihydronicotinamide-A Model for Reduced DPN J. Am. Chem. Soc. **77:** 2261- 2264 (1955).
7. Guenerich, F. P. Brian, W. R. Iwasaki, M., Sari, M. A. Baarnheim, C. Berntsson, P. Oxidation of dihydropyridine calcium channel blockers and analogs by human liver cytochrome P-450 IIIA4. J . Med. Chem.34: 1838-1844 (1991).
8. Guo, K. Thompson, M. J. Reddy, T. R. K. Mutter, R. Chen, B. Mechanistic studies leading to a new procedure for rapid microwave assisted generation of pyridine-3,5-dicarbonitrile libraries. Tetrahedron, **63**: 5300-5311(2007).
9. Karki, R. Thapa, P. Kang, M. J. Jeong, T. C. Namb, J. M. Kim, H. L. Na, Y. Cho, W. J. Kwon,Y. Lee, E. S. Synthesis, topoisomerase I and II inhibitory activity, cytotoxicity, and structure–activity relationship study of hydroxylated 2,4-diphenyl-6-aryl pyridines. Biorg. Med. Chem. **18**: 3066-3077 (2010).
10. Bischhoff, H. Angerbauer, R. Bender, J. Bischoff, E. Faggiotto, A. Petzinna, D. Pfitzner, J. Porter, M. C. Schmidt, D., Thomas, G. Cerivastatin: pharmacology of a novel synthetic and highly active HMG-CoA reductase inhibitor. Atherosclerosis, **135:** 119-130 (1997).
11. Itoh, T. Nagata K. Okada, M. Ohsawa, A. The Aromatization of Hantzsch Dihydropyridines with nitric o xide (NO). Tetrahedron Lett. **36:** 2269-2272 (1995).
12. Shaikh, A. C. Chen, C. Facile and efficient aromatization of 1,4-dihydropyridines with $M(NO_3)_2$-XH_2O,TNCB, TBAP and HMTAI and preparation of deuterium labeled dehydronifedipine from nifedipine-d3. Bioorg. Med. Chem. Lett., **20:** 3664-3668. (2010).
13. Ko, K.J. kim, J. Y. Aromatization of Hantzsch 1,4 – dihydropyridines with magtrieve Tetrahedron Lett. **40:** 3207-3208 (1999).
14. Eynde , J.J.V. Orazio R. D. Van Haverbeke, Y. Potassium permanganate a versatile reagent for the aromatization of Hantzsch 1,4dihydropyridines. Tetrahedron, **50:** 2479-2484 (1994).
15. Phanchgalle, S. P. Choudhary, S. M. Chavan, S. P. Kalkote U R. The oxidation of 4-alkyl and 4-aryl-1,4-dihydropyridines to pyridines with hydrogen peroxide in an ionic liquid J. Chem. Res. Vol. **2004**: 550-551 (2004).
16. Varma, R. S. Kumar, D. Manganese triacetate mediated oxidation of Hantzsch 1,4-dihydropyridines to pyridines. Tetrahedron Lett. **40:** 21-24 (1999).
17. Mashraqui, S. H. Kamik, M. A. Catalytic oxidation of Hanbsch 1,4-dihydropyridines by $RuCl_3$ under oxygen atmosphere. Tetrahedron Lett. **39:** 4895-4898 (1998).
18. Nakamichi, N. Kawashita, Y. Hayashi, M. Oxidative aromatization of 1,3,5-trisubstituted pyrazolines and Hantzsch 1,4-dihydropyridines by Pd/C in acetic acid. Org. Lett., **4:** 3955-3957 (2002).

19. Chai, L. Zhao, Y. Sheng, Q. Liu, Z. Q. Aromatization of Hantzsch 1,4-dihydropyridines and 1,3,5-trisubstituted pyrazolines with HIO_3 and I_2O_5 in water. Tetrahedron Lett., **47**: 9283-9285(2006).
20. Zolfigol, M. A. Bagherzadeh, M. Niknam, K. Shirini, F. Mohammadpoor-Baltore, I. Choghamarana, A. G. Oxidation of 1,4-dihydropyridines under mild and heterogeneous conditions using solid acids. J. Iran. Chem. Soc. **3:** 73-80 (2006).
21. Guengrich, F. P. Bocker, R. H. Cytochrome P-450-catalyzed dehydrogenation of 1,4-dihydropyridines. J. Biol .Chem., **263**: 8168-8175 (1988).
22. Filipan-Litvic, M. Litvic, M., Vinkovic, V. A highly efficient biomimetic aromatization of Hantzsch-1,4-dihydropyridines with t-butylhydroperoxide, catalysed by iron(III) phthalocyanine chloride. Bioorg. Med. Chem. **16**: 9276-9282 (2008).
23. Filipan-Litvic, M. Litvic, M., Vinkovic, V. Rapid, efficient, room temperature aromatization of Hantzsch-1,4-dihydropyridines with vanadium(V) salts: superiority of classical technique versus microwave promoted reaction Tetrahedron, **64**: 10912-10918 (2008).
24. Zolfigol, M A. Safaiee, M. Synthesis of 1,4-Dihydropyridines under solvent –free conditions. Syn. Lett. 827-828 (2004).
25. Alve Figueiredo, M. De Faria, A. L. Das Doress Assis, M. Paulino Oliveria, H. Synthesis by sol–gel process, characterization and catalytic activity of vanadia–silica mixed oxides J Non-Cryst Solids, **351**: 3624-3629 (2005).
26. Murgia, V. Farfan Torres, E. M. Gottifredi, J. C. Sham, E. L. Sol–gel synthesis of V_2O_5-SiO_2 catalyst in the oxidative dehydrogenation of n-butane. Appl. Catal. A, **312**: 134-143 (2006).
27. Piumetti, M. Garrone, E. Dyrbeck, H. Blekkan, E. A. Forni, L. $V2O_5$–SiO_2 systems prepared by flame pyrolysis as catalysts for the oxidative dehydrogenation of propane J. Catal. **256:** 45-61(2008).